LWT - Food Science and Technology 144 (2021) 111230

Contents lists available at ScienceDirect

LWT

journal homepage: www.elsevier.com/locate/lwt

Comparison of Cd(II) adsorption properties onto cellulose, hemicellulose and lignin extracted from rice bran

Qinglan Wu [a,b,c], Mingfei Ren [a,b,c], Xinxia Zhang [a,b,c], Cheng Li [a,b,c], Ting Li [a,b,c], Zhi Yang [d], Zhengxing Chen [a,b,c], Li Wang [a,b,c,*]

[a] Key Laboratory of Carbohydrate Chemistry & Biotechnology Ministry of Education, Jiangnan University, Lihu Road 1800, Wuxi, 214122, China
[b] National Engineering Laboratory for Cereal Fermentation Technology, School of Food Science and Technology, Jiangnan University, Lihu Road 1800, Wuxi, 214122, China
[c] Jiangsu Provincial Research Center for Bioactive Product Processing Technology, Jiangnan University, Lihu Road 1800, Wuxi, 214122, China
[d] School of Food and Advanced Technology, Massey University, Auckland, 0632, New Zealand

ARTICLE INFO

Keywords:
Cellulose
Hemicellulose
Lignin
Adsorption
Cadmium

ABSTRACT

Rice bran, an underutilized by-product obtained from outer rice layers, has received wide interest due to its abundance, eco-friendliness, and low cost. In this research, cellulose, hemicellulose and lignin as the main components of rice bran were fractionated, and their Cd(II) adsorption capacity, behavior and mechanism were further studied. The adsorption capacity of cellulose for Cd(II) was 5.79 mg/g within the equilibrium time of 10 min, which was 1.8 and 3.6 times those of hemicellulose and lignin, respectively. The Cd(II) adsorption onto cellulose exhibited monolayer surface behavior, whilst the heterogeneous adsorption behavior was observed for hemicellulose and lignin. These differences were related to the discrepancy of morphology and chemical composition in three polymers. The multi-hole sticks morphology of cellulose and porous blocky structure of hemicellulose were observed, while lignin showed compact and agglomerated blocky structure. Cellulose had numerous available adsorption sites including the oxygen-containing functional groups, which bonded with Cd (II) driven by chemical interaction. In conclusion, it highlights that cellulose from rice bran has the great potential of being applied as adsorbent for the Cd(II) removal.

1. Introduction

Cadmium (Cd(II)) is considered as one of the most toxic and common metal pollutants with high mobility and biological accumulation, inevitably causing some potential health risks for human (Ding, Jing, Gong, Zhou, & Yang, 2012; Wang et al., 2019). Recently, adsorption, exchange, membrane separation, reverse osmosis, electrodialysis, and chemical precipitation have already been applied to the treatment of heavy metal ions in water bodies (Cui et al., 2016; Naeem et al., 2019). Among all, adsorption is considered as the most promising and effective technology due to its high efficiency, low cost, simple operation and no secondary pollution (Badescu, Bulgariu, Ahmad, & Bulgariu, 2018; Liu, Li, et al., 2020). It was suggested that graphene, mesoporous silica, zeolite, carbon nanofibers could adsorb heavy metal ions from polluted water. However, the high cost and complexity in fabricating those materials limited their wide utilization (Fan et al., 2020).

Natural biopolymers with low cost, simple preparation, hyperreactivity, environmental friendliness, and chemical stability have attracted considerable attention as heavy metal absorbents in recent years. Some authors have studied the adsorption potential, behavior and mechanism of lignocellulosic materials on heavy metal ions (Moubarik & Grimi, 2015). It was reported that biomass from artichoke could remove Cd(II) through biosorption and its maximum adsorption capacity was 27.09 mg/g (Saavedra, Minarro, Angosto, & Fernandez-Lopez, 2019). Similarly, the Cd(II) adsorption performance of peels from litchi, orange, pomegranate and banana could fitted with the Langmuir isotherm (Chen, Wang, Zhao, & Huang, 2018). Besides this, for rice bran, the dominant reaction might be the ion-exchange controlled by mainly lead sorption process and bulk or boundary layer diffusion (Moeinian, Rostami, Rastgoo, & Mehdinia, 2019). Biomasses from flamboyant pods and bush mango seeds can also be utilized as low-cost adsorbents for Cd(II), Pb(II) and Ni(II) removal (Reynel-Avila, Mendoza-Castillo, Olumide, &

* Corresponding author. National Engineering Laboratory for Cereal Fermentation Technology, School of Food Science and Technology, Jiangnan University, Lihu Road 1800, Wuxi, 214122, China.
E-mail addresses: wangli0318@jiangnan.edu.cn, legend0318@hotmail.com (L. Wang).

https://doi.org/10.1016/j.lwt.2021.111230
Received 22 December 2020; Received in revised form 27 February 2021; Accepted 1 March 2021
Available online 2 March 2021

Bonilla-Petriciolet, 2016). The main mechanisms of heavy metal ions biosorption by lignocellulose may include: (i) electrostatic attraction between metal cations and functional groups; (ii) metal ions exchange (such as K(I), Ca(II), Na(I), Mg(II), -COOM, -R-O-M); (iii) chelation of heavy metal by the C═C, C–O, O–H groups and carboxylic acids (Wang, Huang, et al., 2018).

Rice is a staple food for more than half of the global population. Rice bran, composed around 10% of brown rice, is an underutilized by-product in rice processing. Nearly 74 million tonnes of rice bran are gained annually and frequently discarded or used for animal feed (Zhao et al., 2018). Rice bran is a promising lignocellulosic material due to its abundance, cost-effectiveness and biodegradability. Based on a previous work, we have demonstrated that rice bran fiber displayed the maximal Pb(II) binding capacity of 64.07 mg/g in aqueous solution (Wang, Wu, et al., 2018).

Cellulose, hemicellulose and lignin are the main components of rice bran. Cellulose, composed of long cellobiose unbranched chains of D-anhydroglucose units with β-(1,4)-glycosidic bonds, forms the crystalline region of the rice bran cell wall. It is embedded in a matrix of hemicellulose and lignin. Hemicellulose is defined as a heterogeneous group of polysaccharides, characterized by β-(1 → 4)-linked backbones of sugars in an equatorial configuration, while lignin is an amorphous polyphenol polymer (Wen, Niu, Zhang, Zhao, & Xiong, 2017; Ragab et al., 2018). However, based on our best knowledge, there are limited numbers of studies concerning the influence of lignocellulose composition on metal ions adsorption. The progressive removal of hemicelluloses or lignin led to the increase of metal ions (Pb^{2+}, Cd^{2+} and Zn^{2+}) adsorption onto short hemp fibers (Pejic, Vukcevic, Kostic, & Skundric, 2009), as well as iodine, silver ions adsorption onto flax fibers (Lazić et al., 2018). Rice bran cellulose, hemicellulose and lignin have different morphology, chemical composition and structure, especially in nature, quantity and accessibility of functional groups present in the surface (Ciudad-Mulero, Fernández-Ruiz, Matallana-González, & Morales, 2019). It is expected that these differences have a remarkable impact on Cd(II) adsorption capacity and behavior. Comparing the Cd (II) adsorption properties among three components (cellulose, hemicellulose, and lignin) will provide a bright direction for handling rice bran resources.

This work aims to compare the Cd(II) adsorption capacity of the rice bran main components: cellulose, hemicellulose and lignin. The adsorption kinetics, isotherms were examined. The morphological and structural variations of those components before and after Cd(II) adsorption were also evaluated.

2. Materials and methods

2.1. Materials and chemicals

Defatted rice bran was purchased from Jiangsu Ruimu Biological Technology Co., Ltd. (Jiangsu, China). α-Amylase (30000 U/mL) was provided by Genencor Co., Ltd. (Jiangsu, China). Sodium chlorite was purchased from Aladdin Inc. (Shanghai, China). All other chemicals were of analytical grade and bought from Sinopharm Chemical Reagent Co., Ltd. (Shanghai, China).

2.2. Samples preparations

Extraction of cellulose, hemicellulose and lignin was conducted using a modified method according to Qi et al. (2016) and Guo, Zhang, Shu, Zheng, and Gao (2017). The defatted rice bran was treated with 0.3% α-amylase at 95 °C for 30 min, then centrifuged for 10 min at 4000×*g* (LXJ IIB, Anting Ltd., Shanghai, China). The collected solid residues were treated with 4% NaOH solution at 75 °C for 75 min for protein removal. The obtained rice bran fiber was repeatedly washed by deionized water until pH 7, and subsequently washed with 95% ethanol and acetone for twice. Rice bran fiber was suspended in solution containing 0.1 M HCl and 10% $NaClO_2$ at a solid-to-liquid ratio of 1:100 (g/mL), and stirred for 12 h at 25 °C. Then the pH of the solution was adjusted to 7.0 with 1 M NaOH solution, and subsequently centrifuged at 4000×*g* for 10 min. The obtained precipitate was the delignification sample. The delignification sample was suspended in 24% KOH for 2 h before transferring in 10% KOH for 16 h. After centrifugation at 10000×*g* for 10 min, the supernatant and residue (cellulose) were collected separately. Besides, the pH of the supernatant was adjusted to 5.5 with acetic acid, precipitated with 3 vol of alcohol for 16 h, and centrifuged at 4000×*g* for 10 min to collect the residue (hemicellulose). For lignin extraction, rice bran fiber was suspended in 72% sulfuric acid at a constant solid-to-liquid ratio of 1:10 (g/mL) at 30 °C for 1 h, and 4% sulfuric acid at 121 °C for 1 h. The obtained lignin was washed with deionized water to pH 7. Cellulose, hemicellulose and lignin samples were freeze-dried (Beta 2–8 LD plus, Marin Christ, Co., Ltd, Osterode, Germany) and passed through a 100-mesh sieve. The purities of cellulose, hemicellulose and lignin extracted from rice bran were measured by the methods of Laboratory Analytical Procedure, National Renewable Energy Laboratory (NREL LAP) (Sluiter et al., 2012), which were 86.15%, 92.67% and 80.84%, respectively.

2.3. Adsorption experiments

The cellulose, hemicellulose and lignin were used as adsorbents for the removal of Cd(II) ions in aqueous solutions. Initially, 0.2 g of each adsorbent sample and 20.0 mL $CdCl_2{\cdot}2.5H_2O$ solutions were added to a 100.0 mL glass conical flask. Moreover, the pH values of the mixed solutions were adjusted using 0.1 mol L^{-1} HCL or 0.1 mol L^{-1} NaOH solutions to 7.0. Then, the flask was shaken in a temperature-controlled shaker water bath at 150×*g* and 25 °C. After that, the obtained solution was centrifuged for 10 min at 4000×*g* (LXJ IIB, Anting, Shanghai, China). The concentration of remaining ions in the supernatant was determined using atomic absorption spectrophotometer (AAS, AA-240, Varian Inc., Palo Alto, CA, USA). The determination was repeated three times, and the results were averaged.

In the adsorption kinetics experiments, the $CdCl_2{\cdot}2.5H_2O$ solution concentration was followed by 100 mg/L, and the impact of time on the adsorption capacity was investigated ranging from 0 to 320 min. Besides, for isotherms experiments, 0.2 g adsorbent was added in 20 mL of $CdCl_2{\cdot}2.5H_2O$ solution (10–280 mg/L) at different temperatures (ranging from 10 to 40 °C).

The adsorption capacity q_e (mg g^{-1}) was calculated using Eq. (1):

$$q_e = \frac{C_0 - C_e}{m} \times V \quad (1)$$

where C_0 and C_e (mg L^{-1}) are the initial and equilibrium concentrations of Cd(II), respectively; V (L) is the volume of the solution; m (g) is the weight of the sample; q_e (mg g^{-1}) means the amount of adsorbed Cd(II) at equilibrium.

2.4. Morphology and chemical characterization

To further characterize samples (cellulose, hemicellulose and lignin) before and after Cd(II) adsorption, 20 g of adsorbents was placed in 2000 mL of 100 mg/L $CdCl_2$ solutions under shaking in a temperature-controlled shaker water bath at 150×*g* for 180 min (25 °C, pH 7) to allow the Cd(II) adsorption. Thereafter, the solution was centrifuged for 10 min at 4000×*g* (LXJ IIB, Anting Co., Ltd, Shanghai, China). The precipitated pellets were collected, freeze-dried and they are regarded as samples after Cd(II) adsorption.

2.4.1. Micromorphology

Scanning electron microscopy (SEM, Quanta 200, FEI Ltd., Eindhoven, Holland) was used to examine the surface morphologies of samples before and after Cd(II) adsorption with voltage and

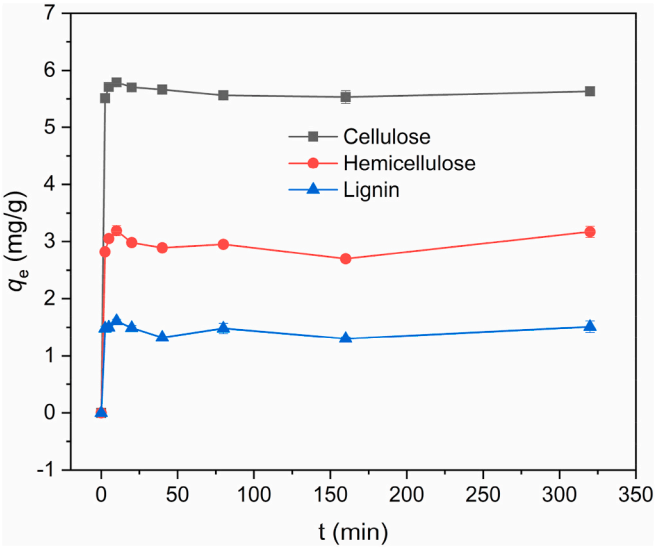

Fig. 1. The effect of contact time on the q_e of Cd(II) adsorption by cellulose, hemicellulose and lignin.

magnification settings of 5.0 kV and 1200, respectively. Prior to analyses, the lyophilized samples were mounted on a circular aluminum stub and sputter coated with gold.

2.4.2. Surface chemical properties

The surface chemical property of samples before and after Cd(II) uptake was explored using X-ray photoelectron spectroscopy (XPS, K-Alpha+, Thermo Fisher Scientific Inc., Waltham, MA, USA). The excitation source was Al kα, and the spectra were collected in the energy range of 0–1300 eV with step size of 1 eV. The deconvolution of the Cd3d, O 1s and C 1s spectra were fitted using Thermo advantage software (version 5.498).

2.4.3. The FTIR spectra

The surface structural features were characterized by a Fourier transformed infrared spectrometer (FTIR, Nicolet iS10, Thermo Fisher Scientific Inc., Waltham, MA, USA). Samples were mixed with spectroscopic grade KBr (1:100, w/w) and pressed into a 1 mm pellet. The spectra were recorded in a range of 4000 to 400 cm^{-1} with a resolution of 2 cm^{-1} and 32 scans.

2.5. Statistical analysis

Statistical analysis was carried out using the Statistical Product and Service Solutions 20.0 analysis program (SPSS, IBM, Chicago, IL, USA), and the differences among trials were evaluated by the Tukey test ($P < 0.05$). All the results reported in the manuscript were repeated at least 3 times.

3. Results and discussion

3.1. Adsorption kinetics

The Cd(II) adsorption kinetics curve of cellulose, hemicellulose and lignin is shown in Fig. 1. The adsorption onto all samples proceeded rapidly at the initial time period ($t < 5$ min). Particularly, within 2.5 min of contact, adsorption capacity of Cd(II) by cellulose sharply increased to 5.51 mg/g. However, the amount of Cd(II) ions adsorbed onto all samples increased slowly at the later time. It could be explained by the numerous vacant sites available on the surface of the samples and a greater driving force by a higher concentration gradient pressure at the initial time (Huang et al., 2020). Furthermore, the equilibrium

Table 1
Kinetics parameters and correlation coefficients for Cd(II) adsorption by different samples.

Samples	Pseudo-first-order			Pseudo-second-order		
	$q_{e,\,cal}{}^{\circ}$	$k_1{}^{\circ}$	R^2	$q_{e,\,cal}{}^{\circ}$	$k_2{}^{\circ}$	R^2
Cellulose	5.654	1.475	0.998	5.650	7.445	0.998
Hemicellulose	2.990	1.165	0.975	2.986	5.756	0.973
Lignin	1.469	1.283	0.957	1.466	5.137	0.957

Note: $q_{e,\,cal}{}^{\circ}$ (mg/g); $k_1{}^{\circ}$ (1/min) and $k_2{}^{\circ}$ (g/mg × min).

adsorption capacities of cellulose, hemicellulose and lignin were 5.79, 3.19 and 1.61 mg/g at 10 min, respectively. After 10 min, the adsorption amount of Cd(II) ions did not change significantly, which is due to that adsorption sites on the surface of adsorbent have been saturated by the Cd(II). The rearrangement or diffusion of Cd(II) ions within the pores of the adsorbent dominated the adsorption behavior (Lucaci, Bulgariu, Ahmad, & Bulgariu, 2020).

To describe the Cd(II) adsorption quantitatively, the pseudo-first-order model (Eq. (2)) and pseudo-second-order model (Eq. (3)) were employed for fitting the adsorption (Tran, You, Hosseini-Bandegharaei, & Chao, 2017):

$$q_t = q_e\left(1 - e^{-k_1 t}\right) \tag{2}$$

$$q_t = \frac{q_e^2 k_2 t}{1 + k_2 q_e t} \tag{3}$$

where q_e (mg g^{-1}) and q_t (mg g^{-1}) are the adsorption amounts of the Cd (II) ions at equilibrium and at any time t (min), respectively; k_1 (min^{-1}) and k_2 (g mg^{-1} min^{-1}) are the rate constants of pseudo-first-order and pseudo-second-order equations, respectively.

Parameters obtained from the two distinct kinetic models for Cd(II) adsorption are listed in Table 1. The pseudo-first-order kinetic equation supposed that the adsorption process was controlled by the chemical interactions which involved a single binding site (Nemeş & Bulgariu, 2016). However, the pseudo-second-order model assumed that chemisorption was due to electron separation or covalent interaction between the adsorbent and the adsorbate (Qu et al., 2019). Regarding to cellulose, hemicellulose and lignin, the similar correlation coefficient (R^2) value of the pseudo-first-order model and pseudo-second-order model was reflected. However, the pseudo-first-order model tallied fitted with kinetics data better than the pseudo-second-order resulting from the closer biosorption capacities calculated from this model ($q_{e,cal}$, mg/g) to the experimental ones ($q_{e,exp}$, mg/g). All of the correlation coefficients were higher than 0.95, so the pseudo-second-order equation was also applicable to the adsorption process. These observations indicated that the adsorption process was mainly controlled by chemical process (Shao et al., 2018).

3.2. Adsorption isotherms

The adsorption isotherms of Cd(II) onto cellulose, hemicellulose, lignin are shown in Fig. 2. The increase in Cd(II) adsorption capacity of cellulose, hemicellulose and lignin with increasing temperature could be attributed to the enhancement of mass transfer dynamics in solution. The molecules were agitated at a relatively larger rate with the increase of thermal energy, resulting in the higher Cd(II) adsorption ability. The endothermicity process infers the association of chemisorption in the adsorption of Cd(II) (Nagarajan & Venkatanarasimhan, 2020). Additionally, the Cd(II) adsorption capacity also increased with the enhancement of the initial Cd(II) ions concentration. Similarly, the adsorption capacity of the Ni(II) was proportional to initial Ni(II) concentration when the amount of chemically modified rice bran fixed reported by Zafar et al. (2015).

To further depict the Cd(II) adsorption process, Langmuir and

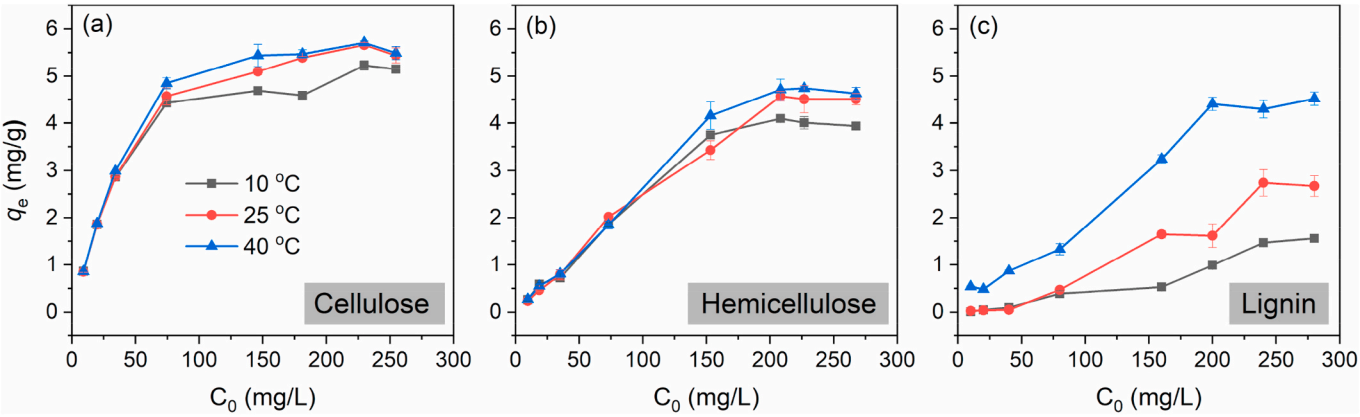

Fig. 2. The effect of initial concentration on adsorption of Cd(II) by cellulose (a), hemicellulose (b) and lignin (c).

Table 2
Langmuir and Freundlich parameters of Cd(II) adsorption at different temperatures.

Samples	Temperature(°C)	Langmuir			Freundlich		
		$Q_{max}°$	$K_L°$	R^2	$1/n$	$K_F°$	R^2
Cellulose	10	4.949	0.359	0.975	0.200	1.847	0.950
	25	5.452	0.278	0.979	0.218	1.856	0.961
	40	5.583	0.347	0.988	0.205	2.034	0.942
Hemicellulose	10	4.439	0.020	0.895	0.630	0.149	0.936
	25	4.635	0.021	0.868	0.711	0.108	0.968
	40	4.729	0.023	0.841	0.689	0.130	0.945
Lignin	10	2.559	0.004	0.810	1.321	0.001	0.961
	25	3.995	0.005	0.795	1.305	0.002	0.920
	40	5.529	0.013	0.847	0.779	0.071	0.949

Note: $Q_{max}°$ (mg/g); $K_L°$ (L/mg); $K_F°$ (mg/g)/(mg/L)$^{-1/n}$.

Freundlich models were used to provide quantitative adsorption information. The Langmuir model assumed the monolayer surface adsorption reaction by applying a fixed number of accessible sites, whilst the Freundlich model described the adsorption behavior on the heterogeneous surfaces. The linear model lacked a reasonable standard with extremely random forms, and any change could lead to diversification of the result (Fan et al., 2020). Therefore, the nonlinear form of Langmuir model (Eq. (4)) and Freundlich model (Eq. (5)) rather than the linear

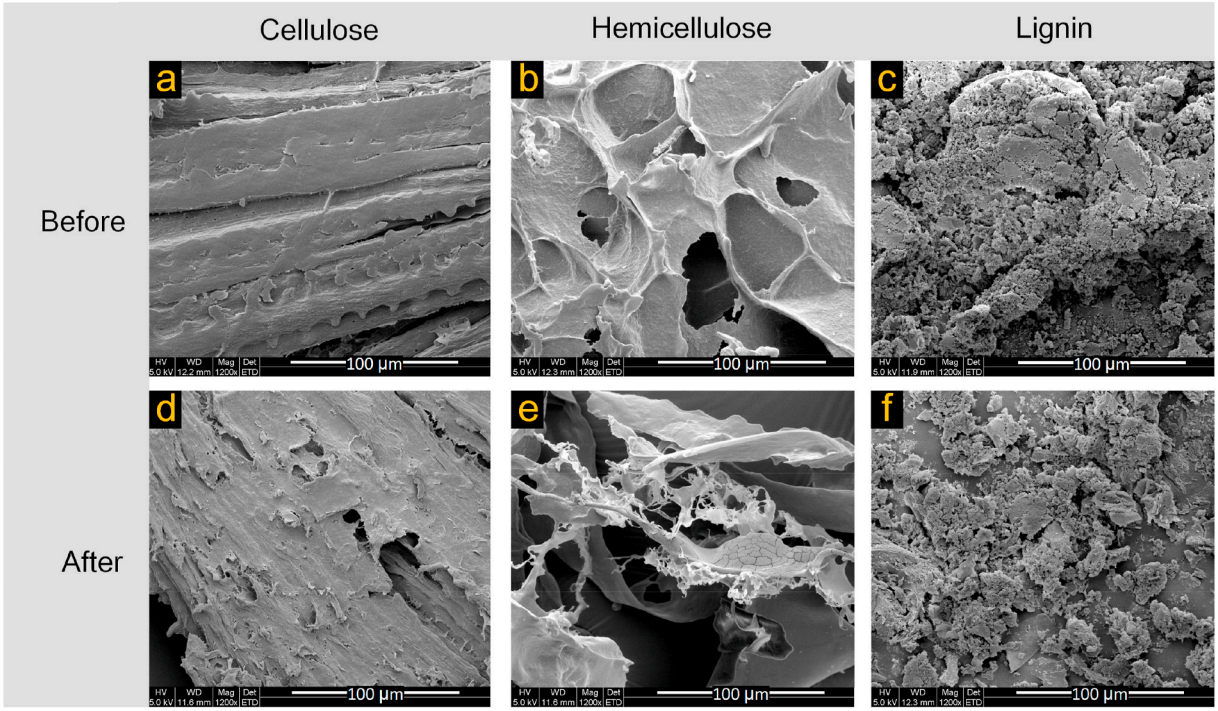

Fig. 3. SEM images of samples before and after the adsorption of Cd(II): cellulose (a, d), hemicellulose (b, e) and lignin (c, f).

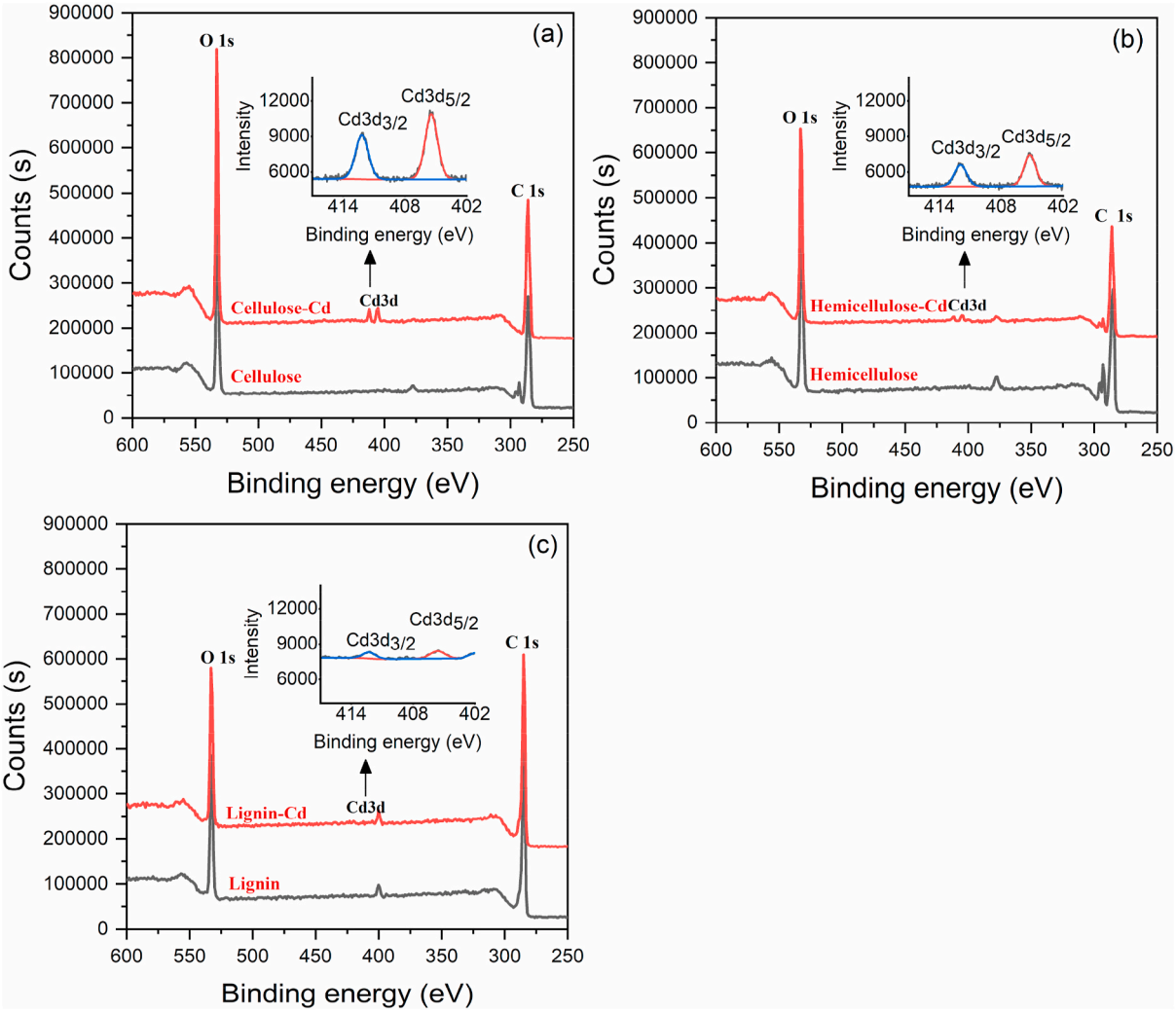

Fig. 4. Wide-scan XPS and deconvoluted Cd3d spectra of cellulose (a), hemicellulose (b) and lignin (c) before and after the adsorption of Cd(II).

method were employed as shown in the following equations:

$$q_e = \frac{K_L Q_{max} C_e}{1 + K_L C_e} \quad (4)$$

$$q_e = K_F \cdot C_e^{1/n} \quad (5)$$

where C_e (mg L^{-1}) is the Cd(II) concentration at equilibrium; q_e (mg g^{-1}) is the adsorption amounts of the Cd(II) ions at equilibrium; Q_{max} (mg g^{-1}) is the maximum adsorption capacity; K_L (L mg^{-1}) is the Langmuir constant corrected with the affinity between an adsorbent and Cd(II); K_F (mg g^{-1})/(mg L^{-1}) $^{-1/n}$ is the Freundlich constant.

The isotherm fitting parameters are listed in Table 2. The Langmuir isotherm of cellulose displayed the higher R^2 value (0.975–0.988), suggesting the better fitness of the model to depict the adsorption processes of Cd(II). This observation indicated that adsorption was fairly uniformly distributed on the surface of cellulose. However, the Langmuir model of hemicellulose and lignin was unable to fit the experimental data well, while the Freundlich model did predict well the Cd(II) adsorption. It is suggested a multi-molecular layer adsorption process. The different fitting result for three adsorbents may be correlated to their different structural features in aqueous solution. Cellulose is a linear homopolymer composed of glucose with β-1,4-glucosidic linkages. Thereafter, the adsorption energy was homogeneously distributed on the surface of cellulose (Mohammadabadi & Javanbakht, 2020). Hemicellulose is a highly branched heteropolysaccharide mainly composed of D-xylose, D-glucose, D-mannose, and lignin is a complex phenolic polymer formed by coumarin, terpineol and sinapyl alcohol. The active adsorption sites on the surface of hemicellulose and lignin were heterogeneously distributed, and adsorption process was not restricted to monolayer formation (Peng, Wu, & Li, 2020; Liu, Liu, et al., 2020). $1/n$ values between 0 and 1 imply the identical adsorption process and adsorption energies for all sites, and low values of $1/n$ imply stronger affinity between the adsorbent and Cd(II) ions (Halysh et al., 2020). The value of $1/n$ had the following order: cellulose < hemicellulose < lignin, indicating that the Cd(II) adsorption capacity onto cellulose and hemicellulose was higher than lignin. Additionally, $1/n$ values obtained of the cellulose and hemicellulose implied favorable Cd (II) adsorption, as they ranged from 0 to 1.

3.3. Surface morphology

The morphological changes in the adsorbents (cellulose, hemicellulose and lignin) before and after Cd(II) adsorption are presented in Fig. 3a-f. For the cellulose, the morphology of sticks with multi-hole was clearly observed (Fig. 3a). The loose and multi-hole characteristics of cellulose were beneficial for binding Cd(II) ions due to the large specific surface area and the active sites were easily exposed. However, after Cd (II) adsorption, it pointed to the occurrence of a rougher surface due to the diffusion of Cd(II) ions (Fig. 3d). As demonstrated by Qu et al. (2019), after Cd(II) adsorption, the surface of microwave-functionalized

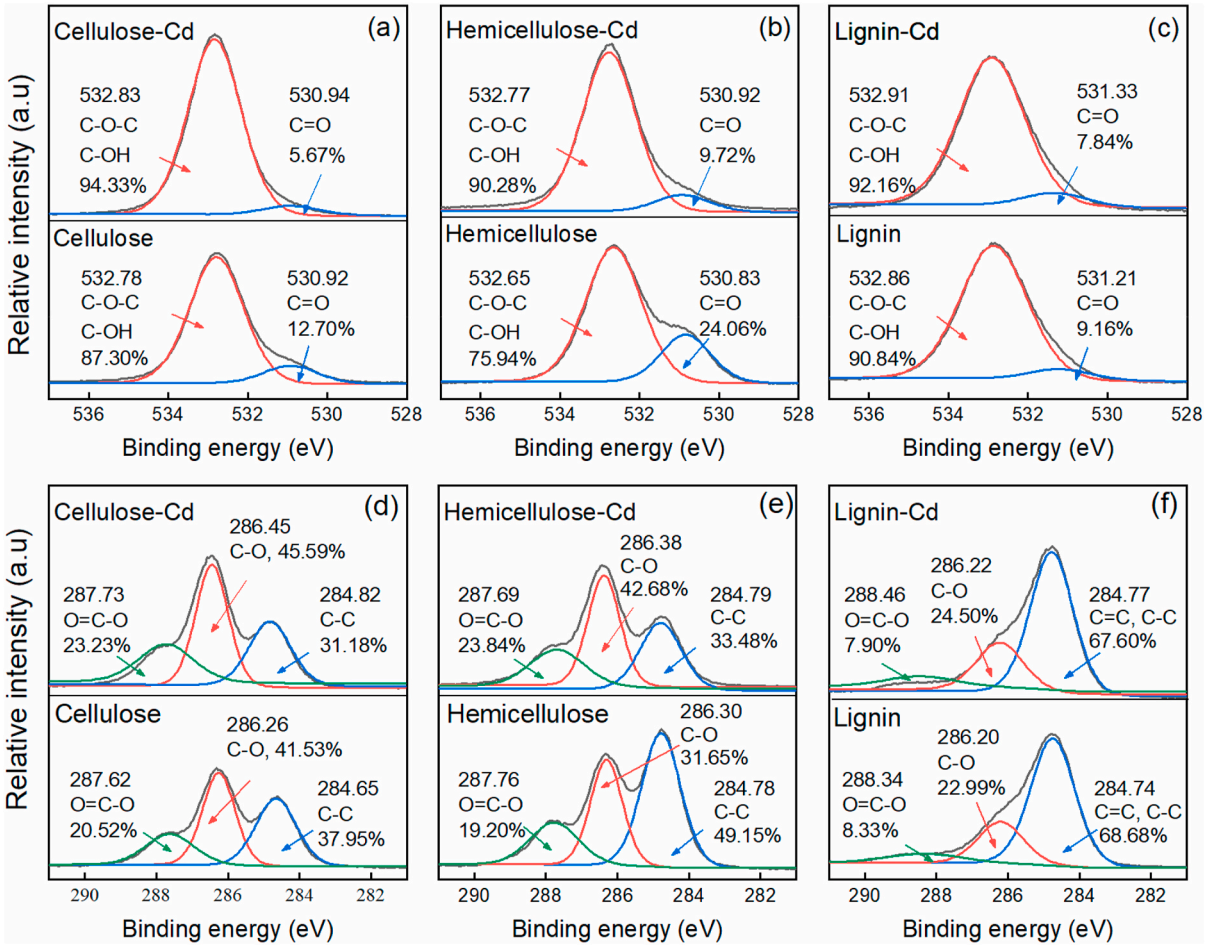

Fig. 5. XPS spectra showing deconvoluted O 1s (a, b, c) and C 1s (d, e, f) of cellulose, hemicellulose and lignin before and after binding with Cd(II).

rice husk cellulose became rougher, which is consistent with the above finding.

Hemicellulose (Fig. 3b) showed a large and porous blocky structure. It was converted to a cleaved face with unfolded laminated structure after Cd(II) adsorption (Fig. 3e). The multi-porous structure of hemicellulose was beneficial for adsorbing Cd(II) ions. After the adsorption of Cd(II) ions, the appearance of some cracks was attributed to the diffusion of Cd(II) ions. A similar result for hemicellulose was found in the study of Alqadami, Khan, Siddiqui, Alothman, and Sumbul (2020), who reported that some cracks were appeared over metals saturated alginate beads (Alqadami et al., 2020). (Wang, Huang, Tu, Ruan, & Lin, 2016) also reported that after Pb(II) adsorption, the soybean insoluble dietary fiber showed unfolded fiber for smaller and thinner particles (Wang et al., 2016).

An irregularly shaped heterogeneous lignin with compact and agglomerated blocky structure was observed (Fig. 3c). The compact and agglomerated characteristics were mainly due to the strong hydrophobic interactions, as well as intramolecular and intermolecular hydrogen bonding (Peng et al., 2020). These features were unfavorable for the adsorption of Cd(II) ions. The morphology of lignin was nearly unchanged after Cd(II) adsorption (Fig. 3f). It was attributed to the fact that the slight amounts of Cd(II) ions were bonded to lignin.

3.4. XPS characterization

Surface functional group compositions and contents of cellulose, hemicellulose and lignin are revealed by the XPS analysis as displayed in Figs. 4 and 5. In Fig. 4a-c, a significant Cd3d binding energy peak for cellulose, hemicellulose and lignin appeared after Cd(II) adsorption, which indicated that the Cd(II) was successfully adsorbed onto samples. What's more, as displayed in the deconvoluted Cd3d spectra, the contents of Cd(II) element followed the order: cellulose > hemicellulose > lignin. The Cd3d XPS spectra could be deconvoluted into two distinct peaks in the range of 402–417 eV. The peak at about 405 eV is ascribed to $Cd3d_{5/2}$, and the peak near 412 eV is attributed to $Cd3d_{3/2}$. The findings indicated that the attaching of Cd(II) to the surface of the adsorbent was affected by surface precipitation or complexation (Huang et al., 2020).

The deconvoluted O 1s spectra of all samples are shown in Fig. 5 (a–c). The peak around 533 eV is attributed to C–O–C and C–OH, and the peak around 531 eV is assigned to C═O (Arun, Perumal, Prakash, Rajesh, & Tamilarasan, 2020; Ma et al., 2019). After Cd(II) adsorption, the binding energy of C–O–C, C–OH and C═O groups increased, indicating that O atoms were electron donors to Cd(II) and the electron density toward O atoms in these groups decreased. Adsorption was probably conducted through the formation of hydroxyl-Cd, carboxyl-Cd, which was basically in line with the reports of Liu et al. (2013) and Wang et al. (2020). The peak area ratio of C═O groups of hemicellulose was higher than cellulose and lignin. It can be explained that hemicellulose contains numerous C═O groups originated from D-galactose, L-arabinose, D-glucuronic acid, 4-O-methyl-D-glucuronic acid, D-galacturonic acid (Yu, Wang, Yu, Wang, & Chi, 2020). Peak area ratios of C═O groups for cellulose, hemicellulose and lignin after adsorption Cd(II) were decreased by 7.03%, 14.34%, 1.32%, respectively. Compared to cellulose and hemicellulose, less C═O groups of lignin formed complexes with Cd(II).

The C 1s spectra of all the samples before and after Cd(II) adsorption are presented in Fig. 5(d–f). The C 1s spectra of cellulose and

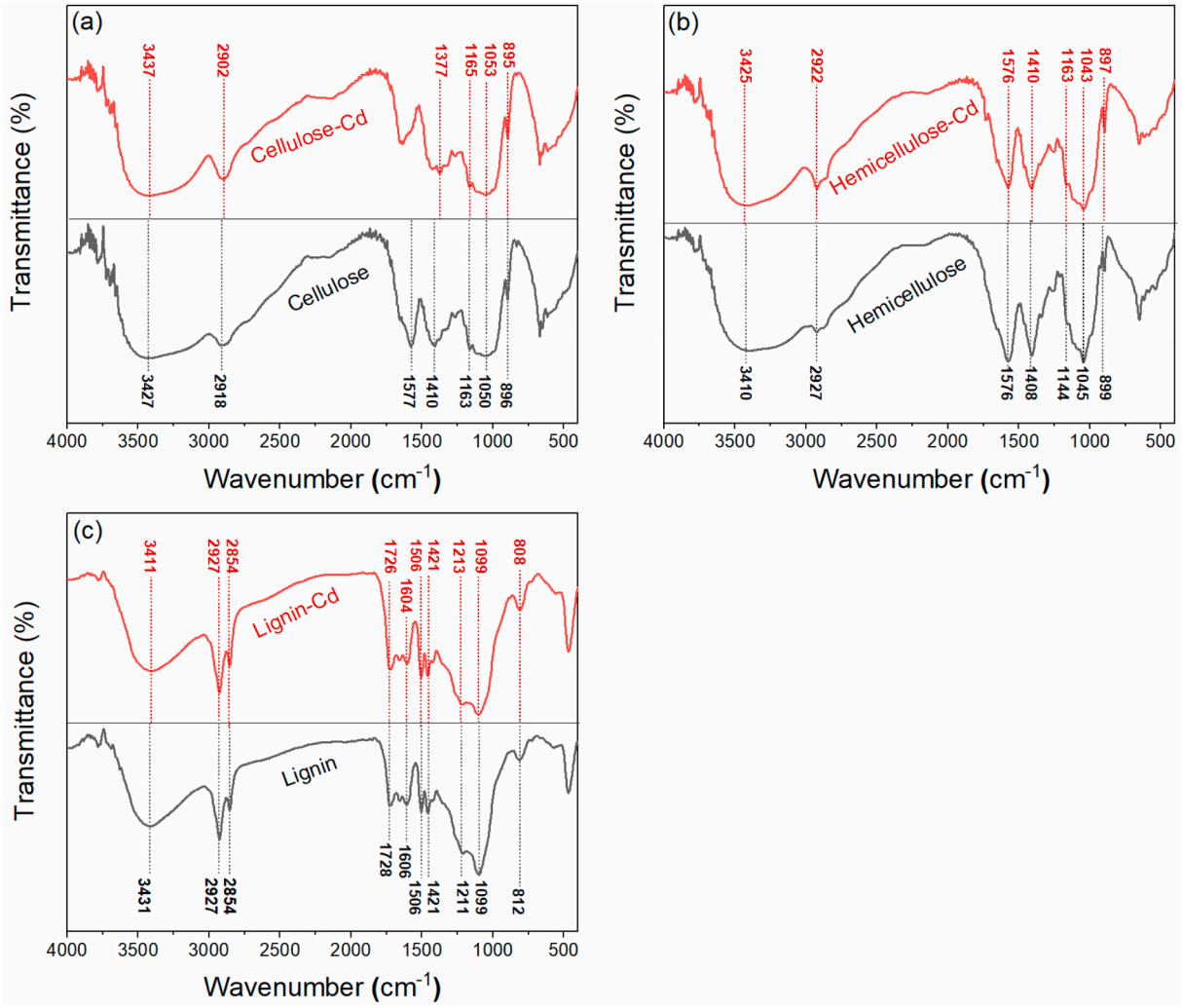

Fig. 6. FTIR spectra of cellulose (a), hemicellulose (b) and lignin (c) before and after the adsorption of Cd(II).

hemicellulose could be divided into three different peaks: (C-I) C–C at ~285 eV, (C-II) C–O (alcohol and ether) at ~286 eV and (C-III) O═C–O (carboxyl and ester) at ~288 eV. In the case of lignin, the C 1s spectrum was also divided into three peaks: (C–I) C═C/C–C around 285 eV, (C-II) C–O (phenolic, alcohol and ether) about 286 eV, and (C-III) O═C–O (carboxyl and ester) around 288 eV (Liu et al., 2013; Park, Wang, Zhou, Mikhael, & DeLaune, 2019). For lignin, the relative content of C═C and C–C peak was reduced after Cd(II) adsorption. It may be related to the Cd–Cπ bonds formed between Cd(II) and C═C groups of coumarin, terpineol or sinapyl alcohol (Chen et al., 2020). Regarding to cellulose, hemicellulose and lignin, the increase in C–O peak was observed after Cd (II) adsorption. It was originated from the reaction between C–OH and $Cd(OH)_2$, which may undergo $Cd(OH)_2 + 2RCOH \rightarrow (RCO)_2Cd + 2H_2O$ (Park et al., 2019). For cellulose and hemicellulose, the relative contents of O═C–O peaks were increased after Cd(II) adsorption, indicating that the surface of samples formed O═C–O. Conversely, the relative content of O═C–O peak decreased after the Cd (II) adsorption onto lignin, implying that the Cd adsorption in lignin involved O═C–O (Chen et al., 2020).

3.5. FT-IR analysis

The functional-group changes of cellulose, hemicellulose and lignin before and after Cd(II) adsorption are shown in Fig. 6a-c. The FTIR spectra of cellulose revealed characteristic adsorption peaks at 3427 cm^{-1} (–OH groups corresponding to the aliphatic moieties), 2918 cm^{-1} (C–H stretching vibration), 1577 cm^{-1} (hydroxyl groups of the adsorbed water), 1410 cm^{-1} (C–H deformation), 1400-1200 cm^{-1} (characteristic vibration of the cellulose skeleton) (Arun et al., 2020), 1163 (C–O–C glycoside bonds asymmetrical stretching), 1105 cm^{-1} (C–OH stretching), 1050 cm^{-1} (C–O–C pyranose ring vibration) (Xiao et al., 2019), and 896 cm^{-1} (β-1,4-glucoside bond) (Chu et al., 2019). The peak at around 3427 cm^{-1} identified as –OH stretching vibration shifted to 3437 cm^{-1} after the adsorption process. The peaks shifting implied the strong interactions between –OH groups and Cd(II) (Li, Zhang, Li, Wang, & Ali, 2016). After Cd(II) adsorption, the peaks of C–O–C, C–OH at 1200-1000 cm^{-1} were all shifted towards the left. This observation may indicate that these functional groups formed complexes with Cd(II) in aqueous solution (Li et al., 2016; Wang et al., 2019).

The characteristic adsorption peaks in hemicellulose were at 3410 cm^{-1}(–OH groups), 2927 cm^{-1} (C–H groups), 1576 cm^{-1} (hydroxyl groups of the adsorbed water) (Ragab et al., 2018), 1408 cm^{-1} (C–H deformation), 1144 cm^{-1} (C–O–C stretching of glycosidic link), 1150-1000 cm^{-1} (C–O, C–C stretching or C–OH bending of xylan) and 899 cm^{-1} (deformation vibration of β–C–H, which was the characteristic band of β-D-xylose) (Hsu, Guo, Chen, & Hwang, 2010; Peng & Wu, 2010). The wavenumber around 3410 cm^{-1} after Cd(II) adsorption was shifted towards the left to a greater extent, indicating the combination of –OH groups with Cd(II) ions (Kołodyńska, Krukowska, & Thomas, 2017). Additionally, the C–O bond in the spectrum of Cd(II) adsorption

shifted from 1045 to 1043 cm^{-1} on account of the coordination of O with Cd(II) (Fakhre & Ibrahim, 2018).

For lignin, the typical peaks were observed at 3431 cm^{-1} (–OH groups in phenolic and aliphatic structures), 2927 and 2854 cm^{-1} (C–H stretching in methyl and methylene groups and methoxy groups), 1728 cm^{-1} (unconjugated ketone or carbonyl stretching), 1606 and 1506 cm^{-1} (aromatic benzene ring), 1421 cm^{-1} (methoxyl groups), 1211 and 1099 cm^{-1} (alkyl aromatic ethers (Ar–O)), 1000-800 cm^{-1} (aromatic C═O, C–H and C–O out of plane deformation) (Dominguez-Robles et al., 2017). The strong carbon–carbon linkages and aromatic groups were resistant to chemical attack and limited the Cd(II) adsorption (Lazić et al., 2018). The –OH peak after Cd(II) adsorption was shifted towards the right (3411 cm^{-1}), implying that the –OH groups could provide hydrogen bonding when adsorbed Cd(II), thereby the sorption behavior was affected by ion exchange and ligand (Huang et al., 2020; Ma et al., 2019).

4. Conclusions

Characteristics and mechanisms of Cd(II) adsorption onto rice bran fractions of cellulose, hemicellulose and lignin were investigated. The Cd(II) adsorption capacity followed a sequence: cellulose > hemicellulose > lignin. For cellulose, the isotherms of the adsorption process were well fitted by the Langmuir model, implying the monolayer adsorption process. However, the Cd(II) adsorption of hemicellulose and lignin was better described by the Freundlich model, which indicated the multilayer adsorption characteristics. The different Cd(II) adsorption behavior could be attributed to different structures and chemical compositions identified in cellulose, hemicellulose, and lignin. Cellulose exhibited rough, porous structure, and had numerous oxygen-containing functional groups, which were beneficial for the Cd(II) adsorption. However, Lignin had a compact and agglomerated blocky structure, and contained substantial amounts of strong carbon–carbon linkages and aromatic groups, which limited the Cd(II) adsorption. After Cd(II) adsorption, cellulose and hemicellulose pointed to the occurrence of a rougher and more porous surface, whilst the surface morphology of lignin hardly changed. Results from this study proved a strong potential of using cellulose extracted from rice bran for Cd(II) removal in various applications such as water purification.

Author Statement

The authors declare that there are no conflicts of interest.

CRediT authorship contribution statement

Qinglan Wu: Conceptualization, Formal analysis, Writing – original draft. **Mingfei Ren:** Methodology, Validation. **Xinxia Zhang:** Resources, Investigation. **Cheng Li:** Software. **Ting Li:** Data curation. **Zhi Yang:** Writing – review & editing. **Zhengxing Chen:** Resources, Funding acquisition, Supervision. **Li Wang:** Resources, Project administration.

Acknowledgment

The research was supported by the National Key R&D Program of China (2017YDF0401100), Natural Science Foundation of Jiangsu Province (BK20171137), National first-class discipline program of Food Science and Technology (JUFSTR20180203), National Natural Science Foundation of China (No. 32072263), National Natural Science Foundation of China (No. 32001737) and China Postdoctoral Science Foundation (No. 2020M671346).

References

Alqadami, A. A., Khan, M. A., Siddiqui, M. R., Alothman, Z. A., & Sumbul, S. (2020). A facile approach to develop industrial waste encapsulated cryogenic alginate beads to sequester toxic bivalent heavy metals. *Journal of King Saud University Science, 32*(2), 1444–1450.

Arun, V., Perumal, E. M., Prakash, K. A., Rajesh, M., & Tamilarasan, K. (2020). Sequential fractionation and characterization of lignin and cellulose fiber from waste rice bran. *Journal of Environmental Chemical Engineering, 8*(5).

Badescu, I. S., Bulgariu, D., Ahmad, I., & Bulgariu, L. (2018). Valorisation possibilities of exhausted biosorbents loaded with metal ions - a review. *Journal of Environmental Management, 224*, 288–297.

Chen, D., Wang, X., Wang, X., Feng, K., Su, J., & Dong, J. (2020). The mechanism of cadmium sorption by sulphur-modified wheat straw biochar and its application cadmium-contaminated soil. *The Science of the Total Environment, 714*, Article 136550.

Chen, Y., Wang, H., Zhao, W., & Huang, S. (2018). Four different kinds of peels as adsorbents for the removal of Cd (II) from aqueous solution: Kinetics, isotherm and mechanism. *Journal of the Taiwan Institute of Chemical Engineers, 88*, 146–151.

Chu, J., Zhao, H., Lu, Z., Lu, F., Bie, X., & Zhang, C. (2019). Improved physicochemical and functional properties of dietary fiber from millet bran fermented by *Bacillus natto*. *Food Chemistry, 294*, 79–86.

Ciudad-Mulero, M., Fernández-Ruiz, V., Matallana-González, M. C., & Morales, P. (2019). Chapter Two - dietary fiber sources and human benefits: The case study of cereal and pseudocereals. In I. C. F. R. Ferreira, & L. Barros (Eds.), *Advances in food and nutrition research* (Vol. 90, pp. 83–134). Academic Press.

Cui, X., Fang, S., Yao, Y., Li, T., Ni, Q., Yang, X., et al. (2016). Potential mechanisms of cadmium removal from aqueous solution by *Canna indica* derived biochar. *The Science of the Total Environment, 562*, 517–525.

Ding, Y., Jing, D., Gong, H., Zhou, L., & Yang, X. (2012). Biosorption of aquatic cadmium (II) by unmodified rice straw. *Bioresource Technology, 114*, 20–25.

Dominguez-Robles, J., Sanchez, R., Diaz-Carrasco, P., Espinosa, E., Garcia-Dominguez, M. T., & Rodriguez, A. (2017). Isolation and characterization of lignins from wheat straw: Application as binder in lithium batteries. *International Journal of Biological Macromolecules, 104*, 909–918.

Fakhre, N. A., & Ibrahim, B. M. (2018). The use of new chemically modified cellulose for heavy metal ion adsorption. *Journal of Hazardous Materials, 343*, 324–331.

Fan, H., Ma, Y., Wan, J., Wang, Y., Li, Z., & Chen, Y. (2020). Adsorption properties and mechanisms of novel biomaterials from banyan aerial roots via simple modification for ciprofloxacin removal. *Science of the Total Environment, 708*, 134630.

Guo, X. Y., Zhang, T., Shu, S. T., Zheng, W., & Gao, M. T. (2017). Compositional and structural changes of corn cob pretreated by electron beam irradiation. *ACS Sustainable Chemistry & Engineering, 5*(1), 420–425.

Halysh, V., Sevastyanova, O., Pikus, S., Dobele, G., Pasalskiy, B., Gun'ko, V. M., et al. (2020). Sugarcane bagasse and straw as low-cost lignocellulosic sorbents for the removal of dyes and metal ions from water. *Cellulose, 27*(14), 8181–8197.

Hsu, T. C., Guo, G. L., Chen, W. H., & Hwang, W. S. (2010). Effect of dilute acid pretreatment of rice straw on structural properties and enzymatic hydrolysis. *Bioresource Technology, 101*(13), 4907–4913.

Huang, X., Zhao, H., Hu, X., Liu, F., Wang, L., Zhao, X., et al. (2020). Optimization of preparation technology for modified coal fly ash and its adsorption properties for Cd^{2+}. *Journal of Hazardous Materials, 392*, 122461.

Kołodyńska, D., Krukowska, J., & Thomas, P. (2017). Comparison of sorption and desorption studies of heavy metal ions from biochar and commercial active carbon. *Chemical Engineering Journal, 307*, 353–363.

Lazić, B. D., Pejić, B. M., Kramar, A. D., Vukčević, M. M., Mihajlovski, K. R., Rusmirović, J. D., et al. (2018). Influence of hemicelluloses and lignin content on structure and sorption properties of flax fibers (*Linum usitatissimum* L.). *Cellulose, 25*(1), 697–709.

Liu, H., Gao, Q., Dai, P., Zhang, J., Zhang, C., & Bao, N. (2013). Preparation and characterization of activated carbon from lotus stalk with guanidine phosphate activation: Sorption of Cd(II). *Journal of Analytical and Applied Pyrolysis, 102*, 7–15.

Liu, Q., Li, Y., Chen, H., Lu, J., Yu, G., Moslang, M., et al. (2020). Superior adsorption capacity of functionalised straw adsorbent for dyes and heavy-metal ions. *Journal of Hazardous Materials, 382*, 121040.

Liu, M., Liu, Y., Shen, J., Zhang, S., Liu, X., Chen, X., et al. (2020). Simultaneous removal of Pb^{2+}, Cu^{2+} and Cd^{2+} ions from wastewater using hierarchical porous polyacrylic acid grafted with lignin. *Journal of Hazardous Materials, 392*, 122208.

Li, M., Zhang, Z., Li, R., Wang, J. J., & Ali, A. (2016). Removal of Pb(II) and Cd(II) ions from aqueous solution by thiosemicarbazide modified chitosan. *International Journal of Biological Macromolecules, 86*, 876–884.

Lucaci, A. R., Bulgariu, D., Ahmad, I., & Bulgariu, L. (2020). Equilibrium and kinetics studies of metal ions biosorption on alginate extracted from Marine Red Algae Biomass (*Callithamnion corymbosum* sp.). *Polymers, 12*(9), 1–16.

Ma, J., Li, T., Liu, Y., Cai, T., Wei, Y., Dong, W., et al. (2019). Rice husk derived double network hydrogel as efficient adsorbent for Pb(II), Cu(II) and Cd(II) removal in individual and multicomponent systems. *Bioresource Technology, 290*, 121793.

Moeinian, K., Rostami, R., Rastgoo, T., & Mehdinia, S. M. (2019). Application of agricultural wastes of rice to lead removal from aqueous solution, study of equilibriums and kinetics. *Desalination and Water Treatment, 153*, 179–192.

Mohammadabadi, S. I., & Javanbakht, V. (2020). Lignin extraction from barley straw using ultrasound-assisted treatment method for a lignin-based biocomposite preparation with remarkable adsorption capacity for heavy metal. *International Journal of Biological Macromolecules, 164*, 1133–1148.

Moubarik, A., & Grimi, N. (2015). Valorization of olive stone and sugar cane bagasse by-products as biosorbents for the removal of cadmium from aqueous solution. *Food Research International, 73*, 169–175.

Naeem, M. A., Imran, M., Amjad, M., Abbas, G., Tahir, M., Murtaza, B., et al. (2019). Batch and column scale removal of Cadmium from water using raw and acid activated wheat straw biochar. *Water, 11*(7).

Nagarajan, D., & Venkatanarasimhan, S. (2020). Kinetics and mechanism of efficient removal of Cu(II) ions from aqueous solutions using ethylenediamine functionalized cellulose sponge. *International Journal of Biological Macromolecules, 148*, 988–998.

Nemeş, L., & Bulgariu, L. (2016). Optimization of process parameters for heavy metals biosorption onto mustard waste biomass. *Open Chemistry, 14*(1), 175–187.

Park, J. H., Wang, J. J., Zhou, B., Mikhael, J. E. R., & DeLaune, R. D. (2019). Removing mercury from aqueous solution using sulfurized biochar and associated mechanisms. *Environmental Pollution, 244*, 627–635.

Pejic, B., Vukcevic, M., Kostic, M., & Skundric, P. (2009). Biosorption of heavy metal ions from aqueous solutions by short hemp fibers: Effect of chemical composition. *Journal of Hazardous Materials, 164*(1), 146–153.

Peng, Y., & Wu, S. (2010). The structural and thermal characteristics of wheat straw hemicellulose. *Journal of Analytical and Applied Pyrolysis, 88*(2), 134–139.

Peng, X., Wu, Z., & Li, Z. (2020). A bowl-shaped biosorbent derived from sugarcane bagasse lignin for cadmium ion adsorption. *Cellulose, 27*(15), 8757–8768.

Qi, J., Li, Y., Masamba, K. G., Shoemaker, C. F., Zhong, F., Majeed, H., et al. (2016). The effect of chemical treatment on the *In vitro* hypoglycemic properties of rice bran insoluble dietary fiber. *Food Hydrocolloids, 52*, 699–706.

Qu, J., Tian, X., Jiang, Z., Cao, B., Akindolie, M. S., Hu, Q., et al. (2019). Multi-component adsorption of Pb(II), Cd(II) and Ni(II) onto microwave-functionalized cellulose: Kinetics, isotherms, thermodynamics, mechanisms and application for electroplating wastewater purification. *Journal of Hazardous Materials, 387*, Article 121718.

Ragab, T. I. M., Amer, H., Mossa, A. T., Emam, M., Hasaballah, A. A., & Helmy, W. A. (2018). Anticoagulation, fibrinolytic and the cytotoxic activities of sulfated hemicellulose extracted from rice straw and husk. *Biocatalysis and Agricultural Biotechnology, 15*, 86–91.

Reynel-Avila, H. E., Mendoza-Castillo, D. I., Olumide, A. A., & Bonilla-Petriciolet, A. (2016). A survey of multi-component sorption models for the competitive removal of heavy metal ions using bush mango and flamboyant biomasses. *Journal of Molecular Liquids, 224*, 1041–1054.

Saavedra, M. I., Minarro, M. D., Angosto, J. M., & Fernandez-Lopez, J. A. (2019). Reuse potential of residues of artichoke (*Cynara scolymus* L.) from industrial canning processing as sorbent of heavy metals in multimetallic effluents. *Industrial Crops and Products*, 141.

Shao, Z. J., Huang, X. L., Yang, F., Zhao, W. F., Zhou, X. Z., & Zhao, C. S. (2018). Engineering sodium alginate-based cross-linked beads with high removal ability of toxic metal ions and cationic dyes. *Carbohydrate Polymers, 187*, 85–93.

Sluiter, A., Hames, B., Ruiz, R., Scarlata, C., Sluiter, J., Templeton, D., et al. (2012). *Determination of structural carbohydrates and lignin in biomass. Laboratory Analytical Procedure*. National Renewable Energy Laboratory.

Tran, H. N., You, S. J., Hosseini-Bandegharaei, A., & Chao, H. P. (2017). Mistakes and inconsistencies regarding adsorption of contaminants from aqueous solutions: A critical review. *Water Research, 120*, 88–116.

Wang, R. Z., Huang, D. L., Liu, Y. G., Zhang, C., Lai, C., Zeng, G. M., et al. (2018). Investigating the adsorption behavior and the relative distribution of Cd^{2+} sorption mechanisms on biochars by different feedstock. *Bioresource Technology, 261*, 265–271.

Wang, H., Huang, T., Tu, Z. C., Ruan, C. Y., & Lin, D. (2016). The adsorption of lead(II) ions by dynamic high pressure micro-fluidization treated insoluble soybean dietary fiber. *Journal of Food Science & Technology, 53*(6), 2532–2539.

Wang, R., Wang, T., Dong, T., Zhong, Q., Chen, Z., Feng, W., et al. (2020). Structural interplay and macroscopic aggregation of rice albumins after binding with heavy metal ions. *Food Hydrocolloids, 98*.

Wang, S., Wang, N., Yao, K., Fan, Y., Li, W., Han, W., et al. (2019). Characterization and interpretation of Cd (II) adsorption by different modified rice straws under contrasting conditions. *Scientific Reports, 9*(1), 17868.

Wang, L., Wu, J., Luo, X., Li, Y., Wang, R., Li, Y., et al. (2018). Dynamic high-pressure microfluidization treatment of rice bran: Effect on Pb(II) ions adsorption *in Vitro*. *Journal of Food Science, 83*(7), 1980–1989.

Wen, Y., Niu, M., Zhang, B. J., Zhao, S. M., & Xiong, S. B. (2017). Structural characteristics and functional properties of rice bran dietary fiber modified by enzymatic and enzyme-micronization treatments. *LWT–Food Science and Technology, 75*, 344–351.

Xiao, Y., Liu, Y., Wang, X., Li, M., Lei, H., & Xu, H. (2019). Cellulose nanocrystals prepared from wheat bran: Characterization and cytotoxicity assessment. *International Journal of Biological Macromolecules, 140*, 225–233.

Yu, H., Wang, J., Yu, J. X., Wang, Y., & Chi, R. A. (2020). Adsorption performance and stability of the modified straws and their extracts of cellulose, lignin, and hemicellulose for Pb^{2+}: pH effect. *Arabian Journal of Chemistry, 13*(12), 9019–9033.

Zafar, M. N., Aslam, I., Nadeem, R., Munir, S., Rana, U. A., & Khan, S. U.-D. (2015). Characterization of chemically modified biosorbents from rice bran for biosorption of Ni(II). *Journal of the Taiwan Institute of Chemical Engineers, 46*, 82–88.

Zhao, G., Zhang, R., Dong, L., Huang, F., Tang, X., Wei, Z., et al. (2018). Particle size of insoluble dietary fiber from rice bran affects its phenolic profile, bioaccessibility and functional properties. *LWT–Food Science and Technology, 87*, 450–456.